Meta-analyses

Editor's Choice

Oikos 125: 288–299, 2016
doi: 10.1111/oik.03100

Subject Editor and Editor-in-Chief: Christopher Lortie. Accepted 17 October 2015

Ecological scaling laws link individual body size variation to population abundance fluctuation

Meng Xu

M. Xu (<http://orcid.org/0000-0002-2569-3654>)(mxu@newhaven.edu), Dept of Mathematics and Physics, Univ. of New Haven, 300 Boston Post Road, West Haven, CT 06516, USA.

Scaling research has seen remarkable progress in the past several decades. Many scaling relationships were discovered within and across individual and population levels, such as species–abundance relationship, Taylor's law, and density mass allometry. However none of these established patterns incorporate individual variation in the formulation. Individual body size variation is a key evolutionary phenomenon and closely related to ecological diversity and species adaptation. Using a macroecological approach, I test 57 Long-Term Ecological Research data sets and show that a power-law and a generalized power-law function describe well the mean-variance scaling of individual body mass. This relationship connects Taylor's law and density mass allometry, and leads to a new scaling pattern between the individual body size variation and population abundance fluctuation, which is confirmed using freshwater fish and forest tree data. Underlying mechanisms and implications of the proposed scaling relationships are discussed. This synthesis shows that integration and extension of existing ecological laws can lead to the discovery of new scaling patterns and complete our understanding of the relation between individual trait and population abundance.

Synthesis

Scaling relationships are useful for community ecology as they reveal ubiquitous patterns across different levels of biological organizations. This work extends and integrates two existing scaling laws: Taylor's law and density-mass allometry, and derives a new variance allometry between individual body mass and population abundance. The result shows that diverse individual body size is associated with stable population fluctuation, reflecting the effect of individual traits on population characteristics. Confirmed by several empirical data sets, these scaling relationships suggest new ways to study the underlying mechanisms of Taylor's law and have profound implications for fisheries and other applied sciences.

Fluctuation of population abundance (count of individuals) in time and space is a central topic in ecology. 60 years ago, MacArthur (1955) used population fluctuations in food webs to introduce the stability concept of ecological communities. MacArthur proposed three possible causes for the fluctuations of species populations in nature: time delay in predation, mortality, and environmental variation. In practice, population fluctuation influences species distribution, reproduction, and extinction, which directly impact the health and food supply of human society (Davis et al. 2005, Hsieh et al. 2006). The role of quantitative patterns of population fluctuation has been emphasized in the design of environmental conservation programs and studies of species diversity (Brown et al. 1995).

Body size is one of the essential properties of individual organisms. It has been studied with population abundance (Damuth's law or abundance mass allometry, Damuth 1987, Brown and Maurer 1989, Reuman et al. 2008), species diversity (body size species richness distribution, Brown et al. 1993, Purvis and Harvey 1997), metabolic rate (Kleiber's law or metabolic rate scaling allometry, Kleiber 1932, Schmidt-Nielsen 1997), and other life history traits or environmental variables (Smock 1980, Peters 1986, Martin and Palumbi 1993, Ashton 2002). Various physical models and evolutionary theory have been proposed to explain these patterns (West et al. 1997, Blanckenhorn 2000). Body size variation was mostly studied at the species level instead of the individual level.

The ecological effect of individual variation was brought into attention by several recent studies. Clark (2010) showed that demographic (e.g. fecundity, growth rate) variation among individuals allows high species diversity of forest trees. Bolnick et al. (2011) reviewed that trait (e.g. diet, predator defense) variation among intraspecific individuals leads to changes in demographic characteristics of the population. They also argued that the notion of individual variation has challenged the traditional population dynamics models where intraspecific variation was not considered. Forsman et al. (2015) showed that high color pattern variation among individual moths was associated with stable population abundance. These empirical findings suggest

that a quantitative framework is urgently needed to facilitate our understanding of individual variation and its relation to population abundance.

On the other hand, ecological scaling laws have been a useful tool to study the interplay between individual body size and population abundance. For example, density mass allometry (DMA) states that the mean population density of a species decays as a power-law function of the average individual body mass. Namely, the bigger individuals are rarer. Marquet et al. (2005) and Cohen et al. (2012) independently proposed, and Cohen et al. (2012) confirmed that Taylor's law (Taylor 1961, [TL]) and DMA can be combined to predict the variance of population abundance as a power-law function of the average individual body mass (called variance-mass allometry [VMA]). In the current work, I tested a mean-variance body mass scaling relationship (called mass allometry [MA]) of individuals, and integrated it with TL and DMA to construct a new scaling pattern between individual body mass variation and population abundance fluctuation (called density mass variance allometry [DMVA]). I tested DMVA using fish data of an African lake and oak tree data from a local forest in Northeast America. The four scaling relationships (TL, DMA, MA, DMVA) are described in Table 1 and its caption.

The idea of individual body mass scaling is not new. Hallgrímsson and Maiorana (2000, abbreviated as HM) studied the relationship between relative-size variability and mean body mass of mammal individuals and Giometto et al. (2013, abbreviated as G) showed that the proportional moment of protist individual body size scaled with the mean body size. My work differs substantially from HM and G in the following three aspects. First, the mathematical formulations of body mass scaling in HM and G are different from the mass allometry in the current work. In fact, HM first transformed the individual body size (mass and total length) on logarithmic scale, then calculated the mean and the variance of log(body size) across all individuals within a group; while in the current work, I first calculated the mean and variance of arithmetic (untransformed) body mass across individuals within a group, then transformed the mean and variance to logarithmic scale. Different orders in which logarithm, mean, and variance act on body size yield different formulations. The fitted equations in this work and in HM are respectively

$$\log\ (variance\ (body\ size)) = a + b \times \log\ (mean\ (body\ size)) \quad (1)$$

and

$$variance\ (\log\ (body\ size)) = c + d \times mean\ (\log\ (body\ size)) \quad (2)$$

Applying the first-order delta method (Oehlert 1992) on the variables of Eq. 2 yields

$$mean\ (\log\ (body\ size)) \approx \log\ (mean\ (body\ size))$$

and

$$\begin{aligned} variance\ (\log(body\ size)) &\approx \left(\frac{1}{mean(body\ size)}\right)^2 \\ &\times variance(body\ size) \\ &= CV^2\ (body\ size) \\ &\neq \log(variance(body\ size)) \end{aligned}$$

Here CV is the coefficient of variation. Delta method shows that the independent variables of Eq. 1 and 2 are approximately equal, but their dependent variables differ.

G's body size scaling (Fig. 2C in Giometto et al. 2013) reads as

$$\frac{mean(body\ size^2)}{mean(body\ size)} = e \times (mean(body\ size))^f \quad (3)$$

Recalling that variance(body size) = mean(body size^2) – (mean(body size))^2, Eq. 3 becomes

$$variance\ (body\ size) = e\ (mean\ (body\ size))^{f+1} - (mean\ (body\ size))^2$$

Unless $f = 1$ and $b = 2$, G's body mass scaling (Eq. 3) is mathematically different from the MA studied here (Eq. 1).

Second, HM's data did not specify the spatial or temporal scales or details. Individuals were grouped purely by taxon (e.g. species, family, or order), and spatially or temporally distant individuals may fall into the same group. G examined individuals living in laboratorial controlled cultures. My analysis took a community ecology perspective, and grouped within-taxon individuals (not necessarily conspecifics) of a natural community from the same geographical location or time period. Each group can therefore be considered as a sub-community of living organisms. Third, HM and G studied individuals of mammal and 13 protist species respectively; while my work analyzed individuals from a wider range of taxa, including amphibian, arthropod, bird, fish, mammal, plant, and reptile (Supplementary material Appendix 1 Table A1).

To calculate the mean and the variance of individual body mass, I grouped within-taxon individuals (not necessarily conspecifics) from the same spatial location or time (called a 'block') of a community. Individuals of different ages, sexes,

Table 1. A scaling quartet between the means and variances of individual body mass and population abundance. The two well-known scaling relationships are Taylor's law (TL: variance of population abundance is a power-law function of the mean population abundance) and density mass allometry (DMA: mean population abundance is a power-law function of the mean individual body mass). The two new scaling relationships studied here are mass allometry (MA: variance of individual body mass is a power-law or a generalized power-law function of the mean individual body mass) and density mass variance allometry (DMVA: variance of population abundance is a power-law or a generalized power-law function of the variance of individual body mass).

	Mean		Variance
Individual body mass	Mean individual body mass	**MA** ↔	Variance of individual body mass
	DMA ↕		**DMVA** ↕
Population abundance	Mean population abundance	**TL** ↔	Variance of population abundance

or species were treated equally without distinction. Population abundance was defined as the number of within-taxon individuals within a spatial or temporal replicate (defined in Material and methods) of each block. Then mean and variance of population abundance were calculated across all replicates in the same block.

I showed that TL, DMA, MA and the predicted DMVA linked four statistical parameters that characterize individuals and populations: mean individual body mass, mean population abundance, variance of individual body mass, and variance of population abundance (Table 1). The scope of data and diversity of taxa used in the testing of MA gave promise to its empirical universality, and suggested that the scaling pattern does not necessarily operate under a specific physical or biological mechanism. DMVA revealed that trait variations across different levels of biological organization (i.e. individual and population) were correlated, and provided a new machinery to analyze the ecological consequence of fishing activities for marine stocks.

Material and methods

Analytic framework

Suppose that N individuals of a taxon were grouped into M blocks. Here a block is a spatial (e.g. site, stand, plot, station) or temporal (e.g. date, year) unit within a data set. Among all N_i individuals in block i ($i = 1, 2, \ldots, M$, $N = N_1 + N_2 + \ldots + N_M$), the mean and the variance of individual body size (denoted by B_j, $j = 1, 2, \ldots, N_i$) were respectively

$$mean_i(B) = \frac{\sum_{j=1}^{N_i} B_j}{N_i}$$

and

$$var_i(B) = \frac{\sum_{j=1}^{N_i} (B_j - mean_i(B))^2}{N_i - 1}$$

If block i ($i = 1, 2, \ldots, M$) contained K_i replicates, the N_i individuals of block i can be subdivided into $N_i = N_{i1} + N_{i2} + \cdots + N_{iK_i}$. Here a replicate is a spatial or temporal subunit within a block (e.g. date within a year, plot within a stand) and N_{il} was the local population abundance (count of individuals) of replicate l ($l = 1, 2, \ldots, K_i$) in block i ($i = 1, 2, \ldots, M$). The mean and variance of population abundance (denoted by A) among all K_i replicates of block i were respectively

$$mean_i(A) = \frac{\sum_{l=1}^{K_i} N_{il}}{K_i}$$

and

$$var_i(A) = \frac{\sum_{l=1}^{K_i} (N_{il} - mean_i(A))^2}{K_i - 1}$$

Density mass allometry (DMA) is a power-law relationship between the mean individual body size and the mean population abundance (Damuth 1987). Across the M blocks, DMA is written as

$$mean_i(A) = \alpha (mean_i(B))^{\beta},\ \alpha > 0 \quad (4)$$

Taylor's law (TL) describes the variance of population abundance as a power-law function of the corresponding mean population abundance (Taylor 1961). Across the M blocks, TL is formulated as

$$var_i(A) = a (mean_i(A))^{b},\ a > 0 \quad (5)$$

I propose a mean-variance scaling relationship of individual body size

$$var_i(B) = c (mean_i(B))^{d},\ c > 0 \quad (6)$$

and name Eq. 6 the mass allometry (MA). I combine Eq. 4–6 into a new scaling relationship between the variance of population abundance and the variance of individual body size.

$$var_i(A) = a (mean_i(A))^{b} = a (\alpha (mean_i(B))^{\beta})^{b}$$
$$= a\alpha^{b} (mean_i(B))^{\beta b} = a\alpha^{b} \left(\left(\frac{\mathrm{var}_i(B)}{c} \right)^{\frac{1}{d}} \right)^{\beta b} = \frac{a\alpha^{b}}{c^{\frac{\beta b}{d}}} (\mathrm{var}_i(B))^{\frac{\beta b}{d}} \quad (7)$$

I name the derived power-law relationship (Eq. 7) the density mass variance allometry (DMVA). Since a, α and c are all positive, the sign of its power exponent $\beta b / d$ determines the behavior of this individual–population variability relationship. As the individual variation of body size increases, population abundance fluctuates less when $\beta b / d < 0$ and more when $\beta b / d > 0$.

Statistical analysis of the four scaling relationships

For each of the four scaling relationships described in Eq. 4–7, the corresponding independent variable and dependent variable were transformed to logarithmic scale ($\log = \log_{10}$ throughout). A least-squares linear regression model was fitted to the transformed variables to test their linearity on the log-log scale (power law), and a least-squares quadratic regression model was fitted to test their curvilinearity (generalized power law).

For example, when testing MA (Eq. 6) in a data set, the taxon-specific means and variances of individual body mass for each block i were calculated and logarithmically transformed and fitted by the least-squares equations across all M blocks ($i = 1, 2, \ldots, M$),

$$\log (var_i(B)) = \log (c_1) + d_1 \log (mean_i(B)) \quad (8)$$

and

$$\log (var_i(B)) = \log (c_2) + d_2 \log (mean_i(B)) + e_2 [\log (mean_i(B))]^2 \quad (9)$$

For each test of MA, p-values of d_1 and e_2, coefficients of determination (R^2), and Akaike information criteria (AIC) of Eq. 8 and 9 were computed. ΔAIC was defined as the AIC of Eq. 9 minus the AIC of Eq. 8. If e_2 was not statistically different from 0 ($p \geq 0.05$) but d_1 was statistically different from 0 ($p < 0.05$), then Eq. 8 was selected as the better model and the power-law form of MA (Eq. 6)

was confirmed. If e_2 was statistically different from 0, then Eq. 9 was selected as the better model and the generalized power-law form of MA was confirmed. If neither e_2 nor d_1 significantly differed from 0, then the model with a smaller AIC was favored and selected. Regression parameter estimates were reported in the Supplementary material Appendix 1 Table A1. All model statistics were computed in R ver. 3.2.0 (< www.r-project.org >).

Denote the statistically favored model (power law or generalized power law) of DMA, TL, MA and DMVA by F_1, F_2, F_3 and F_4 respectively,

$\log(mean_i(A)) = F_1(\log(mean_i(B)))$

$\log(var_i(A)) = F_2(\log(mean_i(A)))$

$\log(var_i(B)) = F_3(\log(mean_i(B)))$ or $\log(mean_i(B)) = F_3^{-1}(\log(var_i(B)))$

$\log(var_i(A)) = F_4(\log(var_i(B)))$

Here F_3^{-1} denotes the inverse function of F_3. I composed F_2, F_1 and F_3^{-1} to predict the form and the parameters of DMVA as

$$\log(var_i(A)) = F_2 \circ F_1 \circ F_3^{-1}(\log(var_i(B))) \quad (10)$$

Here "o" means function composition. The predicted formula (Eq. 10) and its coefficients were compared with the corresponding parameters of F_4 estimated from the data.

Data sets

To test MA, I searched and downloaded taxon-specific (not necessarily conspecific) individual body mass data from Long-Term Ecological Research (LTER) network (2015) using the keywords 'body mass' and 'individual weight'. A complete list of data sets and their citations with DOI are provided in the Supplementary material Appendix 1 Table A1. Individuals that were pooled from multiple studies (under different experimental or environmental conditions) or not randomly sampled (e.g. physiological study using selected predator specimen) were deleted. Data with recaptured or unidentifiable individuals (e.g. plant root, algae), or averaged individual weight or biomass measure (e.g. in g cm^{-2}) were not used in the analysis. Individual body mass was measured by the weight (μg, g or kg) of each individual organism.

For each remaining data set, all individuals of the studied taxon were grouped into blocks defined by the spatial and temporal variables separately. For individuals sampled at multiple times (e.g. dates) in different geographical areas (e.g. stands, plots, islands), each level of the temporal variables (e.g. same date) defined a block, and a mean and a variance of body mass were calculated across all individuals within each such block, representing the average and variation of individuals' body masses at a particular time. Similarly, each level of the spatial variables (e.g. same location) defined a block, and a mean and a variance of body mass were calculated across all individuals within each block, representing the average and variation of individuals' body masses in a particular space. For data sets with only temporal or only spatial variables, the available variables were used to group individuals into blocks. Smallest temporal or spatial units were used to group individuals so that the temporal and spatial effects on body mass variation were completely separated. Temporal or spatial grouping variables were specified in Supplementary material Appendix 1 Table A1. For temporally (spatially) grouped individuals, MA examines whether the time (location) with greater average individual body mass has higher individual mass variation. Use of different weight units does not affect the significance of regressions or the slope estimate of linear regression (Gelman and Hill 2006).

I built the statistical models and estimated the parameters of MA, TL, DMA and DMVA using fish samples from an African lake and oak trees from a deciduous forest in Northeast America.

Individual fish samples were collected from the long-term gillnet sampling program in Lake Kariba, located between Zimbabwe and Zambia. Gillnet fishing was performed almost weekly from 1976 to 2001 at the Lakeside station of Zimbabwe using panels of 11 distinct mesh sizes (51 mm–178 mm with about 12.5 mm increment) (Kolding et al. 2003). For consistency, only fishes caught with uniform catching effort (45.7 by 2 m^2 panel size and 0.5 hanging ratio), bottom-set and multi-filament nets were used. The four most dominant species (common name, scientific name, (count of individuals)) were tigerfish *Hydrocynus vittatus* (31 508), green happy *Serranochromis codringtonii* (29 297), brown squeaker *Synodontis zambezensis* (15 644) and Kariba tilapia *Oreochromis mortimeri* (11 180), from a total of 132 150 individual fishes analyzed in the data. Body mass of each individual fish was measured in weight (g). To calculate the variables needed in the testing of the four scaling relationships, I defined a block as panels of a unique mesh size and a replicate as panels of a unique mesh size in a year. Population abundance was defined as the number of fish caught in a replicate. Mean and variance of individual body mass were calculated across all individual fishes caught by panels of the same mesh size, regardless of species. Mean and variance of population abundance were calculated across all years for panels of a unique mesh size, regardless of species. Supplementary material Appendix 2 Table A1 gives the means and variances used in the analysis. In this case, TL examines whether panels that caught more fishes show higher inter-annual variability in population abundance. DMA tests whether panels that caught smaller individuals caught more fishes. MA tests whether panels that caught larger individual fish on average show higher body mass variation among individuals. DMVA tests whether population abundance fluctuates less in panels with higher individual variation of body mass.

Individual oak trees were sampled in 2007 and 2010 separately from the Black Rock Forest (BRF), Cornwall, NY, USA. In the summer of 2007, 12 experimental plots (75 by 75 m^2 each) were established at the north slope of BRF. Each plot defined a block and was subdivided into nine subplots (25 by 25 m^2 each), each as a replicate. In each subplot, the diameter of breast height (dbh) of individual oak tree was measured if the dbh $\geq$ 2.54 cm (called stem), and the aboveground body mass (ABM, in kg) of each measured tree was calculated using the biomass formula in Brenneman et al. (1978). After a girdling activity in 2008 (Cohen et al. 2012), dbh of each living individual oak stem was measured again in 2010 and the ABM was calculated. In each year of 2007 and 2010, oak population density was defined as the number

of measured oak stems in a subplot. Mean and variance of individual body mass were calculated using ABM across all individual stems within a plot in a given year, regardless of species. Mean and variance of population abundance were calculated across all subplots within a plot in a given year, regardless of species. For each year, TL tests if plots with more trees show higher spatial population variability. DMA tests if plots with smaller individual trees contain more trees. MA tests if individual variation of body mass is higher in plots with larger-sized trees on average. DMVA tests if tree population abundance varies less in plots with higher individual body mass variation. Due to girdling, in 2010, three plots contained no or few live trees and were eliminated from the analysis. Therefore respectively 12 and nine plots were available for regression analysis before and after girdling. Individual tree data can be accessed from the supporting information of Cohen et al. (2012).

Results

Empirical support of mass allometry

I used 57 individual body mass data from 20 Long-Term Ecological Research (LTER) sites (Table 2) to test the functional forms of mass allometry (MA, Eq. 6). In total, the meta-analysis examined 298 811 individuals of at least 869 animal and plant species. The geographical coverage of the data ranged from contiguous United States, Alaska, Mexico, Caribbean to Antarctica (Table 2).

Of the 57 analyzed data sets, individuals were grouped at each level of the temporal variables in 48 sets and again at each level of the spatial variables in 45 sets. In the overall 93 regression tests, 52 (56%) favored the linear model (Eq. 8) and 31 (33%) favored the quadratic model (Eq. 9). In 10 (11%) tests, neither Eq. 8 nor Eq. 9 fitted the data well. Equation 8 and 9 were not substantially different ($|\Delta AIC| \leq 2$) in 58 (62%) tests and Eq. 9 was favored in 34 (37%) of data ($\Delta AIC < -2$). In only one test $\Delta AIC > 2$, meaning that Eq. 9 was substantially worse than Eq. 8. Compared to Eq. 8, Eq. 9 improved the regression R^2 by at least 0.1 in 14 (15%) of the 93 tests. Among the 31 quadratic regressions with statistically significant squared coefficient, four were convex and 27 were concave.

The linear regression slope d_1 (Eq. 8) was significantly different from 0 in 81 of the 93 tests. Among these significant tests, d_1 had a median of 2.11 and a 95% percentile confidence interval (CI) (0.82, 3.83) when individuals were grouped by time periods, and had a median of 2.19 and a 95% percentile CI (1.12, 3.44) when individuals were grouped by spatial locations (Fig. 1a). The wider CI of d_1 for temporally grouped individuals showed that MA was more varied across time than across space, an indication of the demographic stochasticity (e.g. age structure, growth rate) in individual body mass. Under both groupings, the median of R^2 of the significant linear regressions was about 0.7 (Fig. 1b). The slope estimate of d_1 and linear regression R^2 varied widely when the number of blocks and number of individuals per block were small (Fig. 1c–f), at which R^2 reached the lowest values. All regression statistics were reported in Supplementary material Appendix 1 Table A1.

Data analysis of the four scaling relationships

Using fish data from Lake Kariba and oak tree data from Black Rock Forest, I tested the four scaling relationships (MA, TL, DMA, DMVA), and compared the parameters of DMVA estimated from the data and predicted using Eq. 10.

For the Lake Kariba fish data, the four scaling relationships were visually clear (Fig. 2). Regression models were fitted and their statistics were reported in Table 3. Linear model was selected for MA and TL, and quadratic model was selected for DMA and DMVA. The log-log plot of DMA showed slight concavity when mean individual weight was small, indicating underestimation in the number of fishes (Fig. 2c). This may be attributed to two reasons. First,

Table 2. 57 LTER individual body mass data-sets with LTER sites and locations, taxonomic kingdom, number of species and individuals, and average number of blocks per data set.

LTER sites	No. of data sets	Geographical coverage	Kingdom	Total no. of species	Total no. of individuals	Average no. of blocks per data set
AND	1	western United States and Mexico	Plantae	45	10614	649
ARC	4	Alaska	Animalia, Plantae	59	19776	156
BNZ	2	interior Alaska	Animalia, Plantae	6	2840	92
CAP	2	Arizona and northern Mexico	Animalia, Plantae	5	417	38
CDR	5	Minnesota	Animalia, Plantae	108	2935	48
CWT	5	southern Appalachian	Animalia, Plantae	46	10161	29
FCE	1	southern Florida	Plantae	2	282	70
GCE	1	coastal Georgia	Plantae	4	967	14
HFR	3	north central Massachusetts	Animalia, Plantae	32	1776	128
JRN	2	southern United States and Mexico	Animalia	37	8955	336
KBS	2	Michigan	Plantae	>24	14412	41
KNZ	1	Kansas	Animalia	1	5723	19
LUQ	2	northeast Puerto Rico	Animalia	55	1651	39
NTL	12	Wisconsin	Animalia	312	108104	111
NWT	1	Colorado	Animalia	21	3372	406
PAL	2	Antarctica	Animalia	2	8427	201
PIE	3	coastal Massachusetts	Animalia, Plantae	25	67053	27
SEV	3	New Mexico	Animalia, Plantae	47	19800	562
SGS	2	Colorado	Animalia	13	2912	222
VCR	3	coastal Virginia	Animalia	25	8634	220

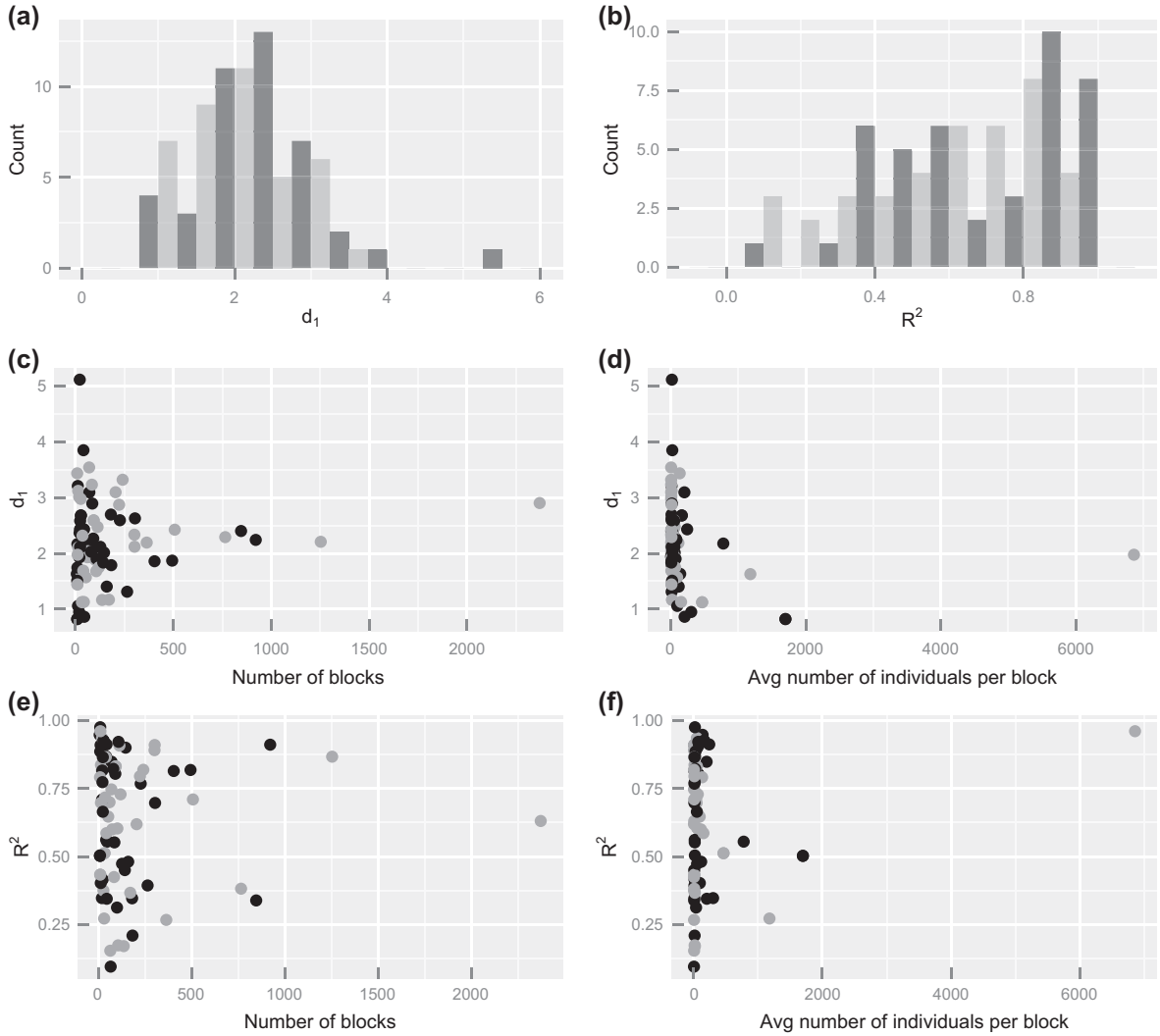

Figure 1. Point estimates of d_1 and R^2 of 81 statistically significant linear regressions for mass allometry (Eq. 8). Black and grey colors indicate respectively that within-taxon individuals were grouped by temporal and spatial variables. (a) Histogram of the point estimate of d_1. (b) Histogram of regression R^2. (c) Point estimate of d_1 against number of blocks. (d) Point estimate of d_1 against average number of individuals per block. (e) R^2 against number of blocks. (f) R^2 against average number of individuals per block.

some small fishes were not individually recorded during the sampling, causing the underestimation of their abundance in numbers. Second, it is possible that small fishes were hiding in shallow areas to avoid predation, therefore not present at the fishing location. Nevertheless, slope of the fitted linear regression of DMA was not significantly different from −1 (95% normal CI = (−1.29, −0.91)), which implied that the product of number of fish and individual fish weight for each size class was a constant. This suggested that the total energy was preserved across the fish communities of different body sizes (White et al. 2007).

Using the formulae of statistically favored models for TL and DMA,

$$\begin{aligned}\log(var(A)) &= -0.66 + 1.98 \times \log(mean(A)) \\ &= -0.66 + 1.98 \times [1.29 + 2.09 \\ &\quad \times \log(mean(B)) - 0.58 \times (\log(mean(B)))^2] \\ &= 1.89 + 4.14 \times \log(mean(B)) - 1.15 \\ &\quad \times [\log(mean(B))]^2 \end{aligned} \quad (11)$$

From the best model of MA

$$\log(var(B)) = 1.10 + 1.50 \times \log(mean(B))$$

I derived

$$\log(mean(B)) = -0.73 + 0.67 \times \log(var(B))$$

Substituting the above equation into Eq. 11 yielded

$$\begin{aligned}\log(var(A)) &= 1.89 + 4.14 \times \left[-0.73 + 0.67 \times \log(var(B))\right] \\ &\quad -1.15 \times \left[-0.73 + 0.67 \times \log(var(B))\right]^2 \\ &= -1.75 + 3.87 \times \log\left(var(B)\right) \\ &\quad -0.51 \times \left[\log\left(var(B)\right)\right]^2 \end{aligned} \quad (12)$$

Equation 12 gave the predicted formula and parameters of DMVA. Each coefficient of Eq. 12 fell within the

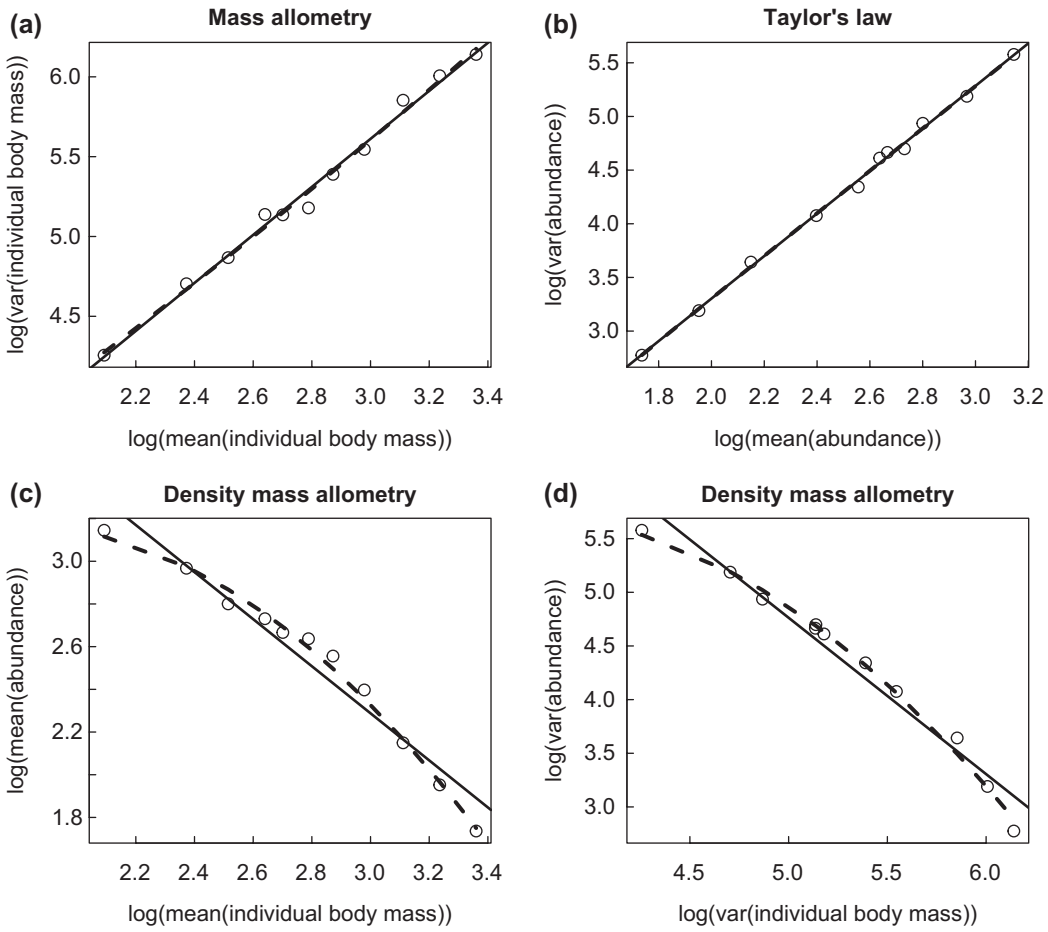

Figure 2. Four scaling relationships tested using Lake Kariba fish sampling data: (a) MA, (b) TL, (c) DMA, and (d) DMVA. Each circle gives the mean and the variance for a block (panels of the same mesh size), calculated across all individuals (for individual fish body mass) or across all years (for fish population abundance). In each panel, the solid line is the fitted least-squares linear regression line and the dashed line is the fitted least-squares quadratic regression line. Regression statistics were reported in Table 3.

corresponding 95% normal CI of DMVA estimated from the fish data (Table 3). Namely, the predicted intercept -1.75 fell within $(-4.44, 4.36)$, predicted linear coefficient 3.87 fell within (1.51, 4.88), and predicted quadratic coefficient -0.51 fell within $(-0.60, -0.28)$.

I repeated the above analysis for the oak tree data in 2007 and 2010 separately.

In all combinations of years and four scaling patterns, the linear model was statistically significant and the quadratic coefficient of quadratic model was not statistically different from 0, with one exception. For DMVA in 2007, the leading coefficient in neither the linear nor the quadratic model was statistically different from 0. However AIC of the linear model (17.16) was smaller than the AIC of the quadratic model (18.05). In all cases, the linear model was favored to the quadratic model (Fig. 3, 4, Table 3). The slope of DMA did not differ significantly from –1 (95% normal CI = $(-1.04, -0.82)$ in 2007 and $(-1.75, -0.65)$ in 2010), which again agreed with the energy-equivalence rule (White et al. 2007).

For trees in 2007, the predicted formula and parameters of DMVA were derived following Eq. 7,

$$\log(var(A)) = \log\left(\frac{a\alpha^{b}}{c^{\frac{\beta b}{d}}}\right) + \frac{\beta b}{d} \times \log\left(var(B)\right)$$
$$= \left[\log(a) + b\log(\alpha) - \frac{\beta b}{d}\log(c)\right] + \frac{\beta b}{d}\log\left(var(B)\right)$$
$$= \left[-1.09 + 2.30 \times 3.87 - \frac{(-0.93)\times(2.30)}{0.49} \times 4.32\right]$$
$$+ \frac{(-0.93)\times(2.30)}{0.49}\log(var(B)) = 26.57 - 4.33 \times \log(var(B))$$

Coefficients predicted from above formula did not fell within the corresponding 95% CI of DMVA estimated from data, but differed slightly from the 95% bounds (Table 3). In particular, the predicted intercept 26.57 was very close to the 95% upper bound of estimated intercept (26.46); the predicted slope -4.33 was very close to the 95% lower bound of estimated slope (-4.31). This discrepancy may be accounted for by the lack of fit in both the linear and quadratic models for DMVA ($R^2 < 0.4$, Table 3).

Similarly, for trees in 2010, the predicted formula and parameters of DMVA were

Table 3. Regression model statistics for the four scaling relationships (*M*A, TL, DMA, DMVA) tested using Lake Kariba fish data and Black Rock Forest oak tree data. Point and interval estimates (in parenthesis) of coefficient, R^2, and AIC of the corresponding linear and quadratic models were included. For each combination of scaling relationship and data set, statistically favored model and the corresponding statistics were indicated in bold face.

Data set	Scaling pattern	Least-squares linear regression				Least-squares quadratic regression				
		Slope	Intercept	R^2	AIC	Quadratic coefficient	Linear coefficient	Intercept	R^2	AIC
Lake Kariba fish	MA	**1.50 (1.40, 1.61)**	**1.10 (0.80, 1.40)**	**0.99**	**−27.91**	0.10 (−0.18, 0.37)	0.98 (−0.56, 2.52)	1.80 (−0.29, 3.90)	0.99	−26.72
	TL	**1.98 (1.91, 2.05)**	**−0.66 (−0.84, −0.48)**	**1**	**−34.50**	−0.01 (−0.19, 0.17)	2.05 (1.17, 2.93)	−0.74 (−1.79, 0.31)	1	−32.54
	DMA	−1.10 (−1.29, −0.91)	5.60 (5.06, 6.13)	0.95	−15.31	**−0.58 (−0.78, −0.38)**	**2.09 (0.98, 3.20)**	**1.29 (−0.22, 2.80)**	**0.99**	**−33.99**
	DMVA	−1.46 (−1.68, −1.24)	12.05 (10.88, 13.22)	0.96	−3.20	**−0.44 (−0.60, −0.28)**	**3.19 (1.51, 4.88)**	**−0.04 (−4.44, 4.36)**	**0.99**	**−21.06**
BRF oak trees	before girding MA	**0.49 (0.22, 0.77)**	**4.32 (3.49, 5.15)**	**0.62**	**−21.99**	0.76 (−0.50, 2.02)	−4.02 (−11.47, 3.44)	10.97 (−0.04, 21.98)	0.69	−22.26
	TL	**2.30 (1.59, 3.02)**	**−1.09 (−1.84, −0.33)**	**0.84**	**−0.34**	0.55 (−3.05, 4.16)	1.06 (−7.11, 9.22)	−0.4067 (−4.92, 4.11)	0.84	1.50
	DMA	**−0.93 (−1.04, −0.82)**	**3.87 (3.54, 4.21)**	**0.97**	**−43.88**	0.19 (−0.34, 0.73)	−2.06 (−5.24, 1.11)	5.54 (0.85, 10.24)	0.97	−42.72
	DMVA	**−2.10 (−4.31, 0.12)**	**13.54 (0.63, 26.46)**	**0.31**	**17.16**	9.40 (−13.46, 32.27)	−112.15 (−379.82, 155.51)	335.44 (−447.53, 1118.41)	0.37	18.05
	after girding MA	**0.53 (0.14, 0.93)**	**4.26 (3.04, 5.47)**	**0.59**	**−11.48**	0.75 (−1.47, 2.97)	−3.98 (−17.31, 9.36)	11.00 (−8.96, 30.95)	0.63	−10.45
	TL	**2.09 (1.29, 2.90)**	**−0.85 (−1.64, −0.05)**	**0.84**	**6.68**	1.43 (−1.92, 4.79)	−0.75 (−7.46, 5.95)	0.45 (−2.69, 3.59)	0.87	7.17
	DMA	**−1.20 (−1.75, −0.65)**	**4.63 (2.95, 6.31)**	**0.79**	**−5.60**	1.18 (−1.84, 4.21)	−8.30 (−26.48, 9.88)	15.24 (−11.98, 42.45)	0.82	−4.87
	DMVA	**−3.28 (−5.95, −0.61)**	**20.46 (4.75, 36.17)**	**0.55**	**16.26**	5.38 (−23.07, 33.82)	−66.83 (−403.11, 269.44)	208.19 (−785.26, 1201.63)	0.56	17.49

$$\begin{aligned}\log(var(A)) &= \log\left(\frac{a d^{b}}{c^{\frac{\beta b}{d}}}\right) + \frac{\beta b}{d} \times \log\left(var(B)\right) \\ &= \left[\log(a) + b\log(a) - \frac{\beta b}{d}\log(c)\right] + \frac{\beta b}{d}\log\left(var(B)\right) \\ &= \left[-0.85 + 2.09 \times 4.63 - \frac{(-1.20)\times(2.09)}{0.53} \times 4.26\right] \\ &\quad + \frac{(-1.20)\times(2.09)}{0.53}\log(var(B)) = 28.94 - 4.72 \\ &\quad \times \log(var(B))\end{aligned}$$

Coefficients from the predicted formula fell within the corresponding 95% CI of DMVA estimated from data (Table 3). Namely, predicted intercept 28.94 fell within (4.75, 36.17) and predicted slope − 4.72 fell within (− 5.95, − 0.61).

To summarize, in all three data sets, the predicted form of DMVA matched the statistically favored model of DMVA tested using data. Moreover, parameters of the statistically favored model of DMVA estimated from data were reasonably predicted from TL, DMA, and MA (Eq. 10). The analytic connection between the four scaling patterns was confirmed using the fish and tree data.

Discussion

The body mass variance observed among individuals can be attributed to variations in many demographic and environmental variables, such as life stages, sex differences, species diversity, climatic conditions and food resources. My analysis showed that the majority of long-term ecological research data sets (~90%) obeyed a power-law or a generalized power-law mass allometry (MA). This finding provided a functional description of the individual body mass variation. It is worthwhile to note that when the generalized power law (Eq. 9) was favored for MA, the majority of tests showed that log(variance of body mass) was a concave function of log(mean body mass) (27/31 = 87%), indicating that individual body mass variation saturated as the average individual body mass became large. This makes sense biologically because, for within-taxon individuals, body growth rate decreases dramatically as they reach sexual maturity (Charnov 1993, Angilletta et al. 2004), consequently survived individuals of large body sizes will approximate a unified maximum body size, henceforth reducing individual variation.

In a general sense, the mass allometry (MA) can be considered as Taylor's law (TL) applied to individual body mass because they both describe variance as a function of the mean. In this work I distinguished these two scaling relationships by treating MA as an individual-level pattern and TL as a population-level pattern. Nevertheless, MA and TL resembled in their forms and parameters. On one hand, their shared power-law forms indicated that population abundance and individual body size may share some intrinsic properties, one of which is the skewness in the distributions of interspecific population abundance (Brown 1984, Brown et al. 1995) and individual body size (Gardezi and Silva 1999, Kozłowski and Gawelczyk 2002, Knouft and Page 2003, Smith and Lyons 2011), although the skewness is not universal (Gouws et al. 2011). Recently, it has been shown that random samples of a skewed distribution could generate TL (Cohen and Xu

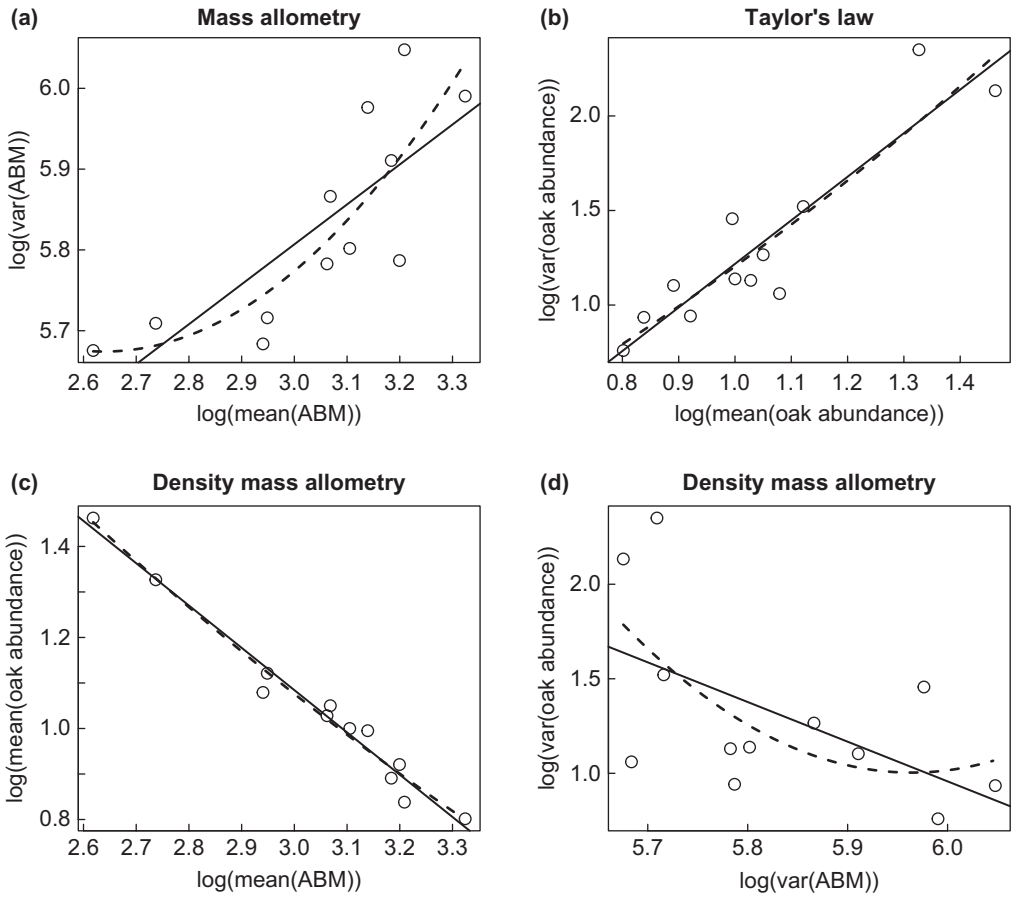

Figure 3. Four scaling relationships tested using BRF oak tree data in 2007 before girdling: (a) MA, (b) TL, (c) DMA, and (d) DMVA. Each circle gives the mean and the variance for a block (plot), calculated across all individuals (for individual tree aboveground body mass) or across all subplots (for tree population abundance). Solid and dashed lines were defined in the legend of Fig. 2. Regression statistics were reported in Table 3.

2015). The theory by Cohen and Xu (2015) can be similarly tested for the individual body size distribution and potentially provide a general statistical explanation for the power-law MA observed here.

On the other hand, using data of hundreds of species from Europe, Taylor and his colleagues (Taylor et al. 1978, Taylor and Woiwod 1980) tested that the slope of TL mostly fell between 1 and 2 with an uppermost value less than 3 (see Fig. 7 in Taylor et al. 1978, Fig. 2 in Anderson et al. 1982 and Fig. 2 in Keil et al. 2010). My meta-analysis showed that the slope of MA fell between 0.82 and 3.83 with a maximum slope of above 5 (Fig. 2a). Compared to TL, the wider range in the slopes of MA may be caused by the different underlying mechanisms of body size and abundance, or merely a reflection of the different geographical coverages and number of species used in the testing of MA (North America, Central America and Antarctica, ~900 species, Table 2) and TL (Great Britain and mainland Europe, ~500 species, Taylor et al. 1978).

My analysis also provided evidence for the validity of MA for intraspecific individuals. In ten intraspecific long-term data sets tested here, eight of them can be described adequately by either the power law (Eq. 8) or the generalized power law (Eq. 9) (Supplementary material Appendix 1 Table A1). This result indicated that interspecific difference is not the sole contributor to individual body mass variation. For intraspecific populations, TL has been widely confirmed (Taylor et al. 1978, Taylor 1984) and density mass allometry (DMA) is mostly well-known as the self-thinning law of plant (Westoby 1984), although the relationship was found weak and polygonal in within-taxon communities of animal (Blackburn et al. 1993) and bird (Nee et al. 1991). Following these observations and the analytic framework derived here, an intraspecific density mass variance allometry (DMVA) seems natural but remains to be tested empirically.

The scaling between individual body size variation and population abundance fluctuation (DMVA) can have profound implications on biological conservation, species extinction and sustainability of food resources. Recently, the impact of fishing on fluctuations of marine population abundance has raised great scientific attentions. Several authors (Hsieh et al. 2006, Anderson et al. 2008, Zhou et al. 2010, Garcia et al. 2012) advocated balanced fishing of various species, ages, sizes, etc. rather than selective fishing, because the latter was found to increase population variability and generate adverse effects on marine ecosystem. Here I use an idealized probability model to demonstrate how DMVA can infer fluctuations in marine fish stocks under different fishing strategies. The main idea is to theorize fishing activities as truncations of a hypothetical body mass distribution.

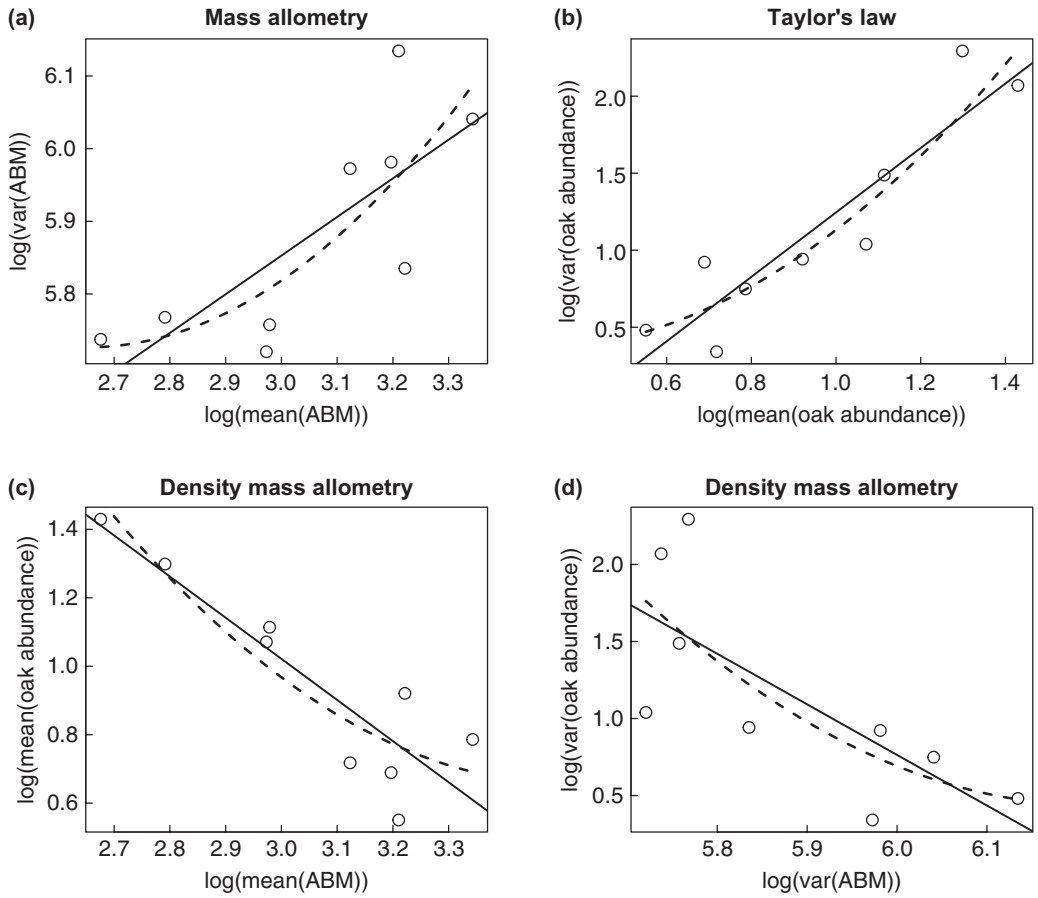

Figure 4. Four scaling relationships tested using BRF oak tree data in 2010 after girdling: (a) MA, (b) TL, (c) DMA, and (d) DMVA. The meaning of each circle was given in the legend of Fig. 3. Solid and dashed lines were defined in the legend of Fig. 2. Regression statistics were reported in Table 3.

These examples are crude in details, but give a simple illustration of the ecological implication of DMVA through changes in the variation of individual body mass. In the following conceptual examples, DMVA is assumed to be valid.

Suppose the individual body mass of a particular marine stock is normally distributed with mean μ and variance σ^2. If selected fishing only harvests fishes above a greater-than-average or below a less-than-average body mass, then the body mass of uncaught individuals can be modeled to follow a truncated normal distribution, with a new variance σ_t^2. It is well known analytically that $\sigma_t^2 < \sigma^2$ (Johnson et al. 1994). According to DMVA, as individual body mass varies less, population abundance fluctuates more. Therefore it implies that fish abundance fluctuates more severely in the exploited stock after selective fishing of adult (upper-truncated normal) or juvenile fish (lower-truncated normal) than in the unexploited stock (normal). Compared to both selective fishing scenarios, balanced fishing in proportion to the mass distribution of individual fish is favorable since it does not alter the underlying individual body mass variance and, according to DMVA, does not increase the population fluctuation. This finding agrees with the recent proposal outlined by Garcia et al. (2012).

I continue using the above model to illustrate the similarity and difference of DMVA with the 'variance mass allometry (VMA)' (Marquet et al. 2005, Cohen et al. 2012). VMA states that the variance of population size decreases as a power-law function of the mean individual body mass. Suppose now the fishing strategy changes to target fish of the most abundance, then we can model the exploited stock as a normal distribution truncated around its mean μ (the peak). For simplicity, I assume that the truncated portion was symmetric about μ ($\mu - k\sigma$ to $\mu + k\sigma$, $k > 0$) and all fishes in the truncated body mass classes were harvested. It can be shown that the truncated body mass distribution had mean μ and variance $\sigma^2[1 + 2k\phi(k)/(1-2\,\Phi(k))]$ (Johnson et al. 1994). Here ϕ is the standard normal probability function and Φ is the standard normal distribution function. Since $k > 0$, $\phi(k) > 0$ and $\Phi(k) > 1/2$, $2k\phi(k)/(1 - 2\Phi(k)) < 0$, therefore the truncated distribution always has a variance less than σ^2. One can deduce that harvesting most abundant species would reduce the variation of individual fish body mass, and, according to DMVA, increase fluctuation in the population abundance. Such change cannot be detected by VMA since the mean body mass before and after selective fishing remains as μ.

The theoretical model above depends on the underlying distribution of individual body mass. Using the empirically realistic Pareto power-law distribution (Garcia et al. 2012), I showed that when small fishes are harvested (a lower-truncated Pareto), the variance of individual body mass increases (Supplementary material Appendix 2) and the corresponding

population abundance fluctuates less according to DMVA. Biologically, selective fishing increases mortality rate and disturbs the natural growth of small individuals, which consequently shrinks the age classes, reduces the corresponding population abundance, and decreases the population fluctuation according to TL (smaller population abundance is associated with higher population variability). On the other hand, when large individuals are targeted (an upper-truncated Pareto), I showed that the variance of individual body mass decreases (Supplementary material Appendix 2) and the corresponding population abundance fluctuated more according to DMVA. In this case, the disappearance of large individuals could negatively affect the spawning activity, which consequently leads to increased fluctuation in fry and juvenile population abundances.

In conclusion, this work provided a comprehensive meta-analysis of the mean-variance individual body mass scaling in communities. The existence of mass allometry suggested that Taylor's law applies not only to population abundance or density, but also to functional trait at the individual level. Such finding broadens the applicability of Taylor's law and offers new channels to examine the underlying mechanisms of Taylor's law, which still remain unclear. The predicted scaling between individual body size variation and population abundance fluctuation (DMVA) showed that increased individual variation can stabilize population abundance and decreased individual variation can disturb population abundance. Increased individual body mass variation may enhance population's adaptation to changing environments, protect genetically superior individuals from predation, and facilitate reproduction and breeding, which all have a positive effect on the stability of population abundance. Despite these biological speculations, challenges remain in the search for a general theory of DMVA. For example, DMVA embodies distributions across two distinct biological organizations, thus the univariate statistical theory developed by Cohen and Xu (2015) is not applicable. Future research should address whether the predicted DMVA is a statistical consequence of the combined existing scaling relationships, or it follows certain biological or physical mechanisms.

Acknowledgements – The author thanks Long-Term Ecological Research Network and the contributors for the individual body mass data sets, William S. F. Schuster for the Black Rock Forest oak tree data, and Jeppe Kolding for the Lake Kariba fish sampling data. LTER data contributors (and their supports) are: Andrews Forest LTER (US National Science Foundation [NSF] Grant DEB-0823380, US Forest Service Pacific Northwest Research Station, and Oregon State University), Arctic LTER (NSF Grants DEB-981022, 9211775, 8702328; OPP-9911278, 9911681, 9732281, 9615411, 9615563, 9615942, 9615949, 9400722, 9415411, 9318529; BSR 9019055, 8806635, 8507493), Bonanza Creek LTER (NSF Grants DEB-0620579, DEB-0423442, DEB-0080609, DEB-9810217, DEB-9211769 and DEB-8702629, USDA Forest Service, Pacific Northwest Research Station [Agreement # RJVA-PNW-01-JV-11261952-231]), Cedar Creek LTER (NSF Grants DEB-0620652 and DEB-1234162, Cedar Creek Ecosystem Science Reserve, and the University of Minnesota), Central Arizona-Phoenix LTER (NSF Grants BCS-1026865, DEB-0423704 and DEB-9714833), Coweeta LTER (NSF Grants DEB-1440485, DEB-0823293, DEB-9632854 and DEB-0218001), Florida Coastal Everglades LTER (NSF Grants DEB-1237517, DBI-0620409 and DEB-9910514), Forest Science Data Bank (Department of Forest Science, Oregon State University, and the U.S. Forest Service Pacific Northwest Research Station, Corvallis, Oregon), Georgia Coastal Ecosystems LTER (NSF Grants OCE-9982133, OCE-0620959 and OCE-1237140), Harvard Forest LTER (NSF Grants DEB- 0080592, DEB-0620443, DEB-1237491), Jornada Basin LTER (NSF Grant DEB-0618210), Kellogg Biological Station LTER (NSF Grant DEB-1027253 and Michigan State University AgBioResearch), Konza Prairie LTER (NSF Grants DEB-0218210 and DEB-0823341), Luquillo LTER (NSF Grants DEB-9705814, DEB-0080538, DEB-0218039, BSR-8811902, DEB-9411973, DEB-0963447, DEB-0620910 and DEB-1239764, U.S. Forest Service, and the University of Puerto Rico), Moorea Coral Reef LTER (NSF Grant OCE-0417412), Niwot Ridge LTER (NSF Grant DEB-1027341), North Temperate Lakes LTER (NSF Grant DEB-1440297), Palmer LTER (NSF Grants OPP-9011927, OPP-9632763 and OPP-0217282), Plum Island Ecosystems LTER (NSF Grants OCE-9726921, OCE-0423565, OCE-1058747 and OCE-1238212), Sevilleta LTER (NSF Grants DEB-9634135, DEB-0236154, DEB-0832652 and DEB-0936498), Shortgrass Steppe LTER (NSF Grant DEB-1027319), and Virginia Coast Reserve LTER (NSF Grants BSR-8702333-06, DEB-9211772, DEB-9411974, DEB-0080381 and DEB-0621014). This work is based on a modified version and not the original data and documentation distributed by the data owners. The author declares no conflict of interest.

AUTHORSHIP: MX designed and performed research, analyzed the data, and wrote the paper.

References

Anderson, C. N. K. et al. 2008. Why fishing magnifies fluctuations in fish abundance. – Nature 452: 835–839.

Anderson, R. M. et al. 1982. Variability in the abundance of animal and plant species. – Nature 296: 245–248.

Angilletta Jr., M. J. et al. 2004. Temperature, growth rate and body size in ectotherms: fitting pieces of a life-history puzzle. – Integr. Comp. Biol. 44: 498–509.

Ashton, K. G. 2002. Patterns of within-species body size variation of birds: strong evidence for Bergmann's rule. – Global Ecol. Biogeogr. 11: 505–523.

Blackburn, T. M. et al. 1993. The relationship between abundance and body size in natural animal assemblages. – J. Anim. Ecol. 62: 519–528.

Blanckenhorn, W. U. 2000. The evolution of body size: what keeps organisms small? – Q. Rev. Biol. 75: 385–407.

Bolnick, D. I. et al. 2011. Why intraspecific trait variation matters in community ecology. – Trends. Ecol. Evol. 26: 183–192.

Brenneman, B. B. et al. 1978. Biomass of species and stands of West Virginia hardwoods. – In: Pope, P. E. (ed.), Proc. Central Hardwood Forest Conf. II. Purdue Univ., West Lafayette, IN, pp. 159–178.

Brown, J. H. 1984. On the relationship between abundance and distribution of species. – Am. Nat. 124: 255–279.

Brown, J. H. and Maurer, B. A. 1989. Macroecology: the division of food and space among species on continents. – Science 243: 1145–1150.

Brown, J. H. et al. 1993. Evolution of body size: consequences of an energetic definition of fitness. – Am. Nat. 142: 573–584.

Brown, J. H. et al. 1995. Spatial variation in abundance. – Ecology 76: 2028–2043.

Charnov, E. L. 1993. Life history invariants: some explorations of symmetry in evolutionary ecology. – Oxford Univ. Press.

Clark, J. S. 2010. Individuals and the variation needed for high species diversity in forest trees. – Science 327: 1129–1132.

Cohen, J. E. and Xu, M. 2015. Random sampling of skewed distributions implies Taylor's power law of fluctuation scaling. – Proc. Natl Acad. Sci. USA. 112: 7749–7754.
Cohen, J. E. et al. 2012. Allometric scaling of population variance with mean body size is predicted from Taylor's law and density-mass allometry. – Proc. Natl Acad. Sci. USA. 109: 15829–15834.
Damuth, J. 1987. Interspecific allometry of population density in mammals and other animals: the independence of body mass and population energy-use. – Biol. J. Linn. Soc. 31: 193–246.
Davis, S. et al. 2005. Fluctuating rodent populations and the risk to humans from rodent-borne zoonoses. – Vector-Borne Zoonot. 5: 305–314.
Forsman, A. et al. 2015. Variable coloration is associated with dampened population fluctuations in noctuid moths. – Proc. R. Soc. B 282: 20142922.
Garcia, S. M. et al. 2012. Reconsidering the consequence of selective fisheries. – Science 335: 1045–1047.
Gardezi, T. and Silva, J. 1999. Diversity in relation to body size in mammals: a comparative study. – Am. Nat. 153: 110–123.
Gelman, A. and Hill, J. 2006. Data analysis using regression and multilevel/hierarchical models. – Cambridge Univ. Press.
Giometto, A. et al. 2013. Scaling body size fluctuations. – Proc. Natl Acad. Sci. USA. 110: 4646–4650.
Gouws, E. J. et al. 2011. Intraspecific body size frequency distributions of insects. – PLoS ONE 6: e16606.
Hallgrímsson, B. and Maiorana, V. 2000. Variability and size in mammals and birds. – Biol. J. Linn. Soc. 70: 571–595.
Hsieh, C.-H. et al. 2006. Fishing elevates variability in the abundance of exploited species. – Nature 443: 859–862.
Johnson, N. L. et al. 1994. Continuous univariate distributions, vol. 1, 2nd edn. – Wiley.
Keil, P. et al. 2010. Predictions of Taylor's power law, density dependence and pink noise from a neutrally modeled time series. – J. Theor. Biol. 265: 78–86.
Kleiber, M. 1932. Body size and metabolism. – Hilgardia 6: 315–353.
Knouft, J. H. and Page, L. M. 2003. The evolution of body size in extant groups of North American freshwater fishes: speciation, size distributions and Cope's rule. – Am. Nat. 161: 413–421.
Kolding, J. et al. 2003. Inshore fisheries and fish population changes in Lake Kariba. – In: Jul-Larsen, E. et al. (eds), Management, co-management or no management? Major dilemmas in southern African freshwater fisheries. Part 2: case studies. FAO, pp. 67–99.
Kozłowski, J. and Gawelczyk, A. T. 2002. Why are species' body size distributions usually skewed to the right? – Funct. Ecol. 16: 419–432.
Long-Term Ecological Research Network 2015. Long-Term Ecological Research Network Data Portal. Available at: <https://portal.lternet.edu/nis/home.jsp>. Last accessed 29 August 2015.
MacArthur, R. 1955. Fluctuations of animal populations and a measure of community stability. – Ecology 36: 533–536.
Marquet, P. A. et al. 2005. Scaling and power-laws in ecological systems. – J. Exp. Biol. 208: 1749–1769.
Martin, A. P. and Palumbi, S. R. 1993. Body size, metabolic rate, generation time, and the molecular clock. – Proc. Natl Acad. Sci. USA. 90: 4087–4091.
Nee, S. et al. 1991. The relationship between abundance and body size in British birds. – Nature 351: 312–313.
Oehlert, G. W. 1992. A note on the delta method. – Am. Stat. 46: 27–29.
Peters, R. H. 1986. The ecological implications of body size. – Cambridge Univ. Press.
Purvis, A. and Harvey, P. H. 1997. The right size for a mammal. – Nature 386: 332–333.
Reuman, D. C. et al. 2008. Three allometric relations of population density to body mass: theoretical integration and empirical tests in 149 food webs. – Ecol. Lett. 11: 1216–1228.
Schmidt-Nielsen, K. 1997. Animal physiology: adaptation and environment, 5th edn. – Cambridge Univ. Press.
Smith, F. A. and Lyons, S. K. 2011. How big should a mammal be? A macroecological look at mammalian body size over space and time. – Phil. Trans. R. Soc. B 366: 2364–2378.
Smock, L. A. 1980. Relationships between body size and biomass of aquatic insects. – Freshwater Biol. – 10: 375–383.
Taylor, L. R. 1961. Aggregation, variance and the mean. – Nature 189: 732–735.
Taylor, L. R. 1984. Assessing and interpreting the spatial distributions of insect populations. – Annu. Rev. Entomol. 29: 321–357.
Taylor, L. R. and Woiwod, I. P. 1980. Temporal stability as a density-dependent species characteristic. – J. Anim. Ecol. 49: 209–224.
Taylor, L. R. et al. 1978. The density-dependence of spatial behaviour and rarity of randomness. – J. Anim. Ecol. 47: 383–406.
West, G. B. et al. 1997. A general model for the origin of allometric scaling laws in biology. – Science 276: 122–126.
Westoby, M. 1984. The self-thinning rule. – Adv. Ecol. Res. 14: 167–225.
White, E. P. et al. 2007. Relationships between body size and abundance in ecology. – Trends. Ecol. Evol. 22: 323–330.
Zhou, S. et al. 2010. Ecosystem-based fisheries management requires a change to the selective fishing philosophy. – Proc. Natl Acad. Sci. USA. 107: 9485–9489.

Supplementary material (Appendix oik-03100 at <www.oikosjournal.org/appendix/oik-03100>). Appendix 1–2.

Oikos 125: 1211, 2016
doi: 10.1111/oik.03694
Editor-in-Chief: Dries Bonte

Erratum

Xu, M. 2016. Ecological scaling laws link individual body size variation to population abundance fluctuation. – Oikos 125: 288–299. doi: 10.1111/oik.03100

In Fig. 2–4, title of panel (d) was mistakenly labeled as 'Density mass allometry', and should be labeled as 'Density mass variance allometry'.

These corrections do not affect the analysis or findings of the associated article. The author apologizes for the confusion caused by these errors.

Meng Xu